JOURNAL OF MATERIALS SCIENCE 31 (1996) 6431–6439

The influence of anneal on the structural and magnetic properties of the electrodeposited thin-film alloy $Cu_{94}Co_6$

H. J. BLYTHE
Physics Department, The University, Sheffield S3 7RH, UK
G. A. JONES
Physics Department, The University, Salford M5 4WT, UK
V. M. FEDOSYUK
Institute of Solid State Physics and Semiconductors of the BeloRussian Academy of Sciences, 220072 Minsk, Belarus

Magnetic measurements have been made in the temperature range 2 to 300 K and in fields up to 5 T on the electrodeposited, thin-film alloy $Cu_{94}Co_6$. The unannealed alloy, which magnetic measurements suggest consists of face-centred cubic (f.c.c.) Co-rich particles in an f.c.c. Cu-rich matrix, exhibits superparamagnetism and has a maximum blocking temperature, as determined from hysteresis loops, of 55 ± 5 K. Low-field susceptibility measurements give an interaction energy of 1.7×10^{-3} eV. Samples have been annealed at temperatures up to 600 °C. The effect of anneal is to produce a strong increase of remanence and maximum blocking temperature, which corresponds to a growth in particle size, together with an increase in the interaction energy. After the final anneal to 600 °C, the blocking temperature is well above 300 K and the sample shows ferromagnetic behaviour. Detailed electron microscopy measurements have also been made in order to determine the structure of the film and its modification on anneal.

1. Introduction

Reports of the phenomenon of "giant magnetoresistance" (GMR) in a range of magnetic multilayer systems have attracted widespread attention. The origin of the GMR depends on the ability to change the relative orientation of magnetic layers separated by non-magnetic spacer layers. More recently, however, GMR has also been observed in granular, inhomogeneous systems composed of two or more immiscible metals, e.g. AgCo [1, 2], CuCo [3–6], AgFe [7]. These materials consist of nanometre-sized, single-domain particles dispersed in a non-magnetic metallic matrix. Although the details of the theory are still controversial, the physical mechanism involves scattering of the conduction electrons at the surfaces of the granules [8–11]; this scattering is spin-dependent due to the spin-split density of states in the magnetic particles [12, 13].

The GMR effect observed in these granular alloys is comparable with the best values obtained in magnetic multilayers [7] and, as a result of the potential technological application of these materials, work on these systems has been the focus of great interest. Up to the present time, however, almost all of these materials have been produced by such relatively complicated and expensive techniques as sputtering [6], mechanical alloying [14], melt-spinning [6], laser-ablation [4] or various high-vacuum deposition methods. In contrast to these methods, we have employed the simple and economic technique of electrodeposition (ED) to produce inhomogeneous films of CuCo, which is one of the most widely investigated alloy systems; CuCo thin film grown by ED have also been reported by Ueda and Ito [15]. One of the advantages of ED is that, in principle, varying the exact conditions of deposition enables us to "fine-tune" the properties of the film to our specific requirements. Here, perhaps, we should also draw attention to the fact that samples produced via the ED route are inhomogeneous immediately after deposition [16, 17]. ED is also a successful route to multilayer production: recently, for example, Alper *et al.* [18] have produced short-period Cu/Co–Ni–Cu superlattices using the technique of ED and Lenczowski *et al.* [19] have observed GMR in Cu/Co multilayers.

There are several important factors which influence the GMR behaviour of heterogeneous films. These include the size, separation and distribution of the magnetic particles in the non-magnetic matrix, together with the composition profile in the vicinity of the interface of the particles. All of these parameters are sensitive, not only to the method of preparation,

0022–2461

but also to the influence of anneal, since in metastable, immiscible systems this generally initiates the precipitation and subsequent growth of the small particles and also affects their composition. Indeed, in most of these systems, the maximum value of GMR is only attained after anneal. Clearly then, it is essential to have a basic understanding of the magnetic behaviour of these materials on anneal.

In earlier papers [16, 17, 20] we have reported on the magnetic behaviour of the thin CuCo films produced by ED and have shown that, even at such a low Co concentration as $Cu_{94}Co_6$, the film does not exhibit pure superparamagnetism (SPM) but that interaction effects have to be considered. In the present paper, we have investigated the influence of anneal on the magnetic properties of the film. Since the physical properties of these films, and fine-particle systems generally, depend strongly upon their method of preparation and the resulting microstructure (see Chantrell *et al.* [21] for a recent discussion of interaction effects in fine-particle systems) we also present the results of detailed electron microscopic investigations made on the samples. We have placed considerable emphasis on the structural investigation of the material since, unlike CuCo films produced by the other techniques mentioned above; samples prepared by ED have received only little attention.

2. Experimental technique

2.1. Sample preparation

The $Cu_{94}Co_6$ films, which were prepared in Minsk, were electrodeposited onto either Al, Cu or ceramic substrates; the ceramic substrates had previously been coated with a non-magnetic layer of NiP. The electrolytic composition was as follows:

$CuSo_4 \cdot 5H_2O$	$30\ g\,l^{-1}$
$CoCl_2 \cdot 6H_2O$	$3.3\ g\,l^{-1}$
H_3BO_3	$6.6\ g\,l^{-1}$
$MgSO_4 \cdot 7H_2O$	$23.3\ g\,l^{-1}$
$CoSO_4 \cdot 7H_2O$	$10\ g\,l^{-1}$
$Na_3C_6H_5O_7 \cdot 5.5H_2O$	$120\ g\,l^{-1}$
$C_6H_4SO_2NHCO$	$1\ g\,l^{-1}$

The electrolyte had a pH of 6.0 and deposition was performed at 20 °C with a current density of 5 mA cm^{-2}. Immediately prior to deposition, the Cu substrates were washed in detergent and then lightly etched in a 5% solution of HCl. The metallic substrates were, in general, of thickness ca. 0.1 mm and films were typically of order 1 μm thick.

2.2. Composition and structure

The film composition was determined in Minsk by both X-ray and chemical analysis [16]. For the X-ray analysis we used CoK_α radiation with a graphite monochromator and a Dron-3M instrument. Transmission electron microscope (TEM) measurements were made using an EMV-1004M machine with an accelerating voltage of 100 keV. In order to prepare samples of uniform thickness, we prepared relatively thick CuCo films and then, after dissolving the Al substrate in a 10% solution of NaOH, thinned the samples by electropolishing in a 50% H_3PO_4 solution.

Additional TEM measurements were also performed in Salford on both unannealed and annealed films using a 300 keV Jeol 3010. This group of samples was prepared for microscopy by ion-milling with the substrate side facing the ion beam. Unfortunately, this preparation technique can induce post-deposition artefacts [22]. Such seemed to be the case here, as thinning did not proceed uniformly, insofar as marked thickness variations resembling "hillocks" of spatial extent up to ca. 1 μm were evident in the microphotographs; this was particularly so for the annealed specimens.

2.3. Magnetic measurements

Magnetic measurements, which were mainly made on films deposited onto Cu substrates, were performed in the temperature range 2–300 K and in fields of up to 5 T using a Quantum Design SQUID magnetometer. Fields were applied in the plane of the film and could be set to an accuracy of $\pm 10^{-6}$ T; temperatures could be controlled to within $\pm 10^{-2}$ K. Measurements of magnetic moment as a function of field for various temperatures were made, together with the technique of zero-field-cooled (ZFC) and field-cooled (FC) low-field susceptibility measurements [17]. In this latter type of measurement, the sample was cooled in zero field from room-temperature to 2 K and then a measuring field of 5 mT was applied; measurements were then made in this constant field whilst the temperature was increased. The sample was then cooled down to 2 K in the same field (5 mT) while, again, measurements were made of the moment.

In order to estimate the diamagnetic contribution of the Cu substrate, an uncoated substrate of known mass was measured. Subsequent measurements on ED films were then corrected for the substrate contribution by weighing the whole sample and then subtracting off an appropriately scaled value for the uncoated substrate. It was assumed that the film itself made a negligible contribution to the total mass. Measurements were made on the film immediately after preparation (no anneal) and then after annealing for 30 minutes at 200, 400 and 600 °C. For these anneals, the samples were sealed-off in quartz ampoules in a vacuum of better than 10^{-3} Pa.

3. Results and discussion

3.1. Composition and structure

A transmission electron diffraction pattern from an unannealed sample is shown in Fig. 1(a), together with a key to the main reflections present. Reflections from at least two f.c.c. phases may be identified with lattice parameters of 0.362 ± 0.002 nm and 0.424 ± 0.002 nm. The former corresponds – within experimental error – to that of Cu (0.3615 nm). The second phase is more problematic in that the estimated lattice constant falls midway between that of Cu_2O (0.4220 nm) and CoO (0.4260 nm) which differ by only 1%. It seems certain

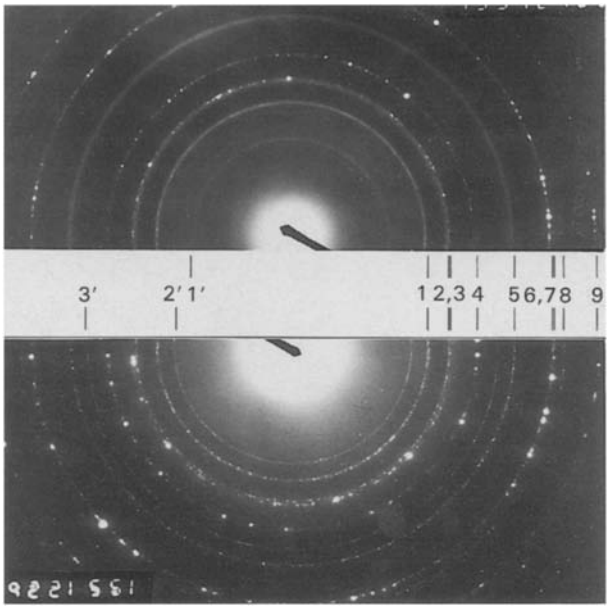

Figure 1 Electron diffraction patterns of (a) "as-received" and (b) annealed films of $Cu_{94}Co_6$. The unprimed reflections are common to both films, namely: Oxide reflections: 1. (1 1 1); 2. (2 0 0); 5. (2 2 0); 7. (3 1 1); 8. (2 2 2). Copper reflections: 3. (1 1 1); 4. (2 0 0); 6. (2 2 0); 9. (3 1 1). The primed reflections are unique to one or other of the films. The annealing temperature was 600 °C.

that the second set of reflections arises from one of these oxides but, in view of the experimental error involved, it is not possible to decide between them. However, the disproportionate content of Cu in the samples naturally favours an oxide of this metal. Cu_2O is a stable oxide whose growth could possibly be promoted in the aqueous environment in which the films were prepared. Since the oxide was not detected with X-ray diffraction, a technique which samples the bulk, it seems more likely that the oxidation is a surface phenomenon, perhaps encouraged by the ion-milling thinning procedure.

Some other comments are worthy of note with regard to Fig. 1(a). The oxide rings are of more uniform intensity than the Cu rings – which are distinctly spotty – suggesting that the grain size of the former is much smaller. It will be noticed from the indexing that some rings of each phase either overlap or have very similar "d" spacings. Consequently, the separation of each phase with dark-field microscopy is rendered more difficult. Finally, even after the identification of Cu and Cu_2O, some low-angle reflections could not be accounted for. The intensity of these rings varied from point to point on the sample.

The failure to observe reflections attributable to either f.c.c. or h.c.p. Co is not surprising in the light of previous work. In his seminal paper Kneller [23] concluded that evaporated films comprise a metastable disordered f.c.c. phase; no distinct Co reflections were observed. More recently, Rabedeau *et al.* [24] could detect the presence of segregated spherical Co clusters in unannealed co-evaporated $Co_{16}Cu_{84}$ films (but not sputtered films) only by small-angle X-ray scattering at grazing incidence; electron microscopy and conventional diffraction techniques proved ineffective. Similarly, Yu *et al.* [25, 26] observed no Co reflections from melt-spun $Co_{15}Cu_{85}$ or Co_5Cu_{95} alloys and Wan *et al.* [22] failed to detect diffraction lines from Fe in FeAg sputtered films. Moreover, since the Co content of our films is so low, it is likely that even if phase segregation were to occur, it would not be detectable with electron diffraction.

Fig. 2(a) is an electron micrograph of an unannealed specimen and reveals some interesting features. Several large areas are seen which have either dominant light- or dark-contrast separated by well-defined boundaries. These gross variations of contrast are not due to thickness gradations, but rather to diffraction contrast. Dark-field microscopy indicates that they are associated with Cu rings and we suggest that they

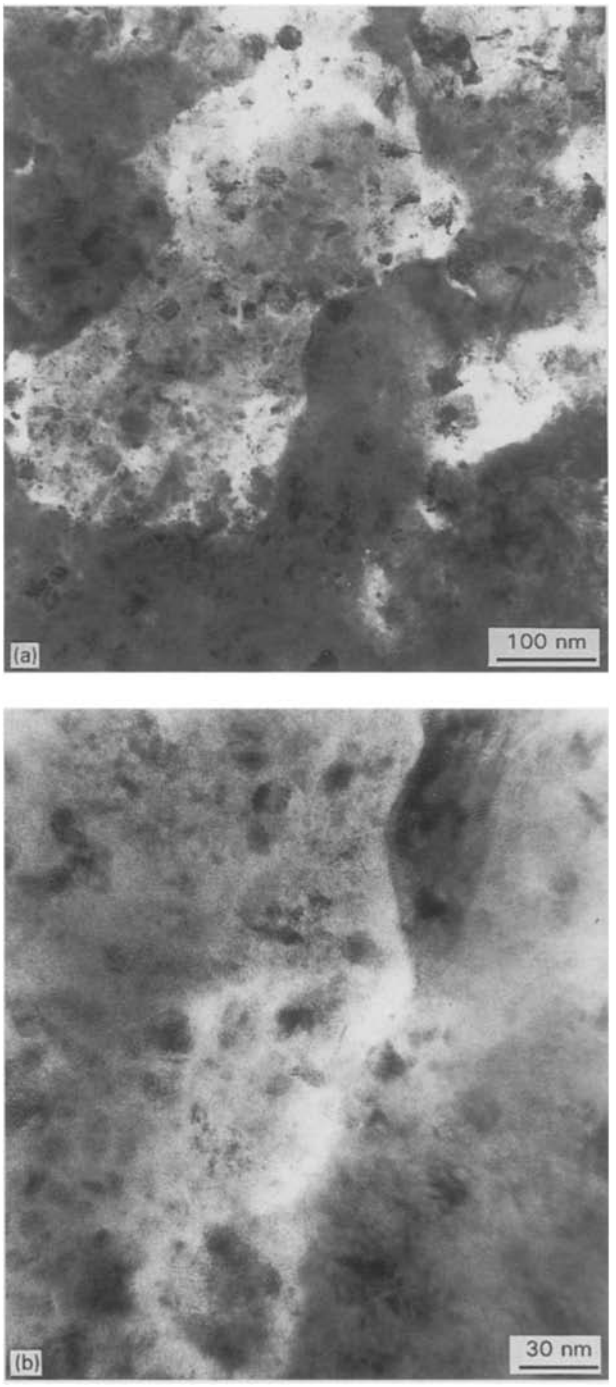

Figure 2 Bright-field micrographs of "as-received" sample of $Cu_{94}Co_6$. The central portion of (a) is shown at higher resolution in (b).

are a reflection of the underlying grain structure of the Cu substrate which, in some areas, is replicated directly into the electrodeposited film. Evidence for this phenomenon has recently been reported by Daniel *et al.* [27]. Such areas possessing some degree of common crystallographic texture would account for the spots on the Cu reflections (Fig. 1(a)). Further confirmation of these ideas comes from high-resolution micrographs which show the direction of lattice planes to be roughly conserved within a particular area of dark or light contrast.

Within the large Cu grains are found smaller features varying in extent up to 50 nm. While it might be tempting to associate these features with clusters of Co or Co-rich material, the factors discussed above preclude this possibility. Their size, irregular shape and strong contrast suggest that they are small crystals rendered visible through conventional diffraction contrast and, indeed, dark-field microscopy shows that they are grains of oxide (Cu_2O). Such a range of grain size is consistent with the continuous nature of the diffraction rings. In Fig. 2(b), at much higher magnification, it can be seen that the edges of the oxide grains are not well defined but somewhat diffuse.

The electron diffraction pattern of an annealed sample is shown in Fig. 1(b) – below that of the unannealed sample in order to facilitate comparison. Again, reflections from the two phases noted previously are present, although it should be remarked that the oxide rings now contain some spots. On the other hand, the prominent, unidentified, low-angle reflections in Fig. 1(a) have vanished, although two other rings with "d" spacings of 0.283 nm and 0.162 nm are present. These correspond, within 1.5%, to the (2 2 0) and (4 2 2) reflections of Co_3O_4, which also has an f.c.c. structure. In view of the comparatively large discrepancy, we do not place undue confidence on this identification, particularly as other rings which might be expected from this phase are absent. As with the as-received samples, the intensity of these extra rings depends on the particular area viewed. Again, no reflections from Co (either f.c.c. or h.c.p.) could be detected.

It proved difficult to prepare uniformly-thin samples from annealed foils; when examined in the microscope, the specimens portrayed a distinctly lumpy or pebbly aspect. This is illustrated in Fig. 3(a) and (b) which is a pair of micrographs taken from a heavily-etched area of material close to the perforation in the foil. An attempt was made to isolate an oxide reflection to give the dark-field image shown in Fig. 3(b). Some prominent oxide particles are revealed in strong contrast: these are larger (>100 nm) and better defined than in the unannealed state, an observation that accords with the spots on the oxide rings. Other, smaller contrast features (down to 1 nm) are also evident, particularly in the dark-field micrograph. These are frequently associated with a larger oxide grain and the presumption must be that they are of this phase rather than, say, a Co cluster. The most obvious reason for the non-uniform thickness is preferential etching of the Cu (*vis-à-vis* oxide) during the ion-milling process.

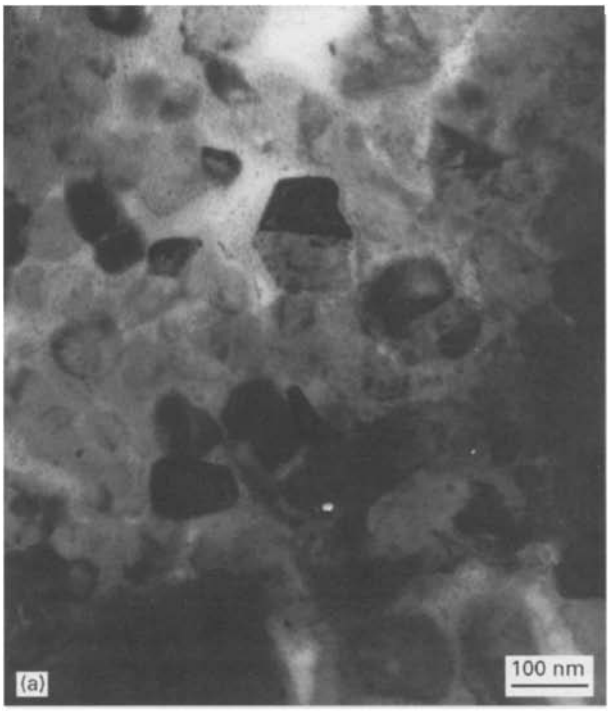

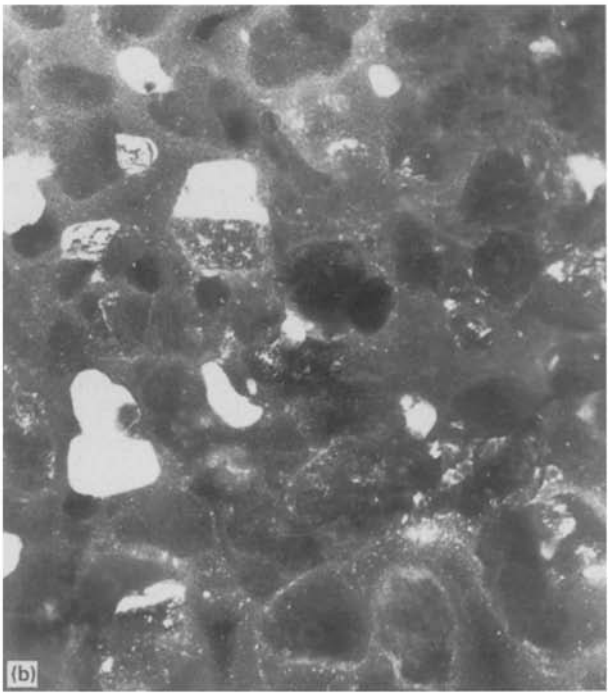

Figure 3 Bright-field (a) and dark-field (b) micrographs of a sample of $Cu_{94}Co_6$ annealed at 600 °C. The particles diffracting in (b) are oxide.

In thicker regions of the specimen, areas of the Cu matrix dominate, as is shown in Fig. 4(a). The large circular patches to the left and right sides of the micrograph are the result of thickness variations. Of more interest are the smaller, weaker contrast features, roughly circular in form and of fairly uniform size (ca. 4 nm), which are clearly visible over the entire micrograph. At higher magnification (Fig. 4(b)) the small patches remain discernable but the lattice planes of the alloy are also resolved. As expected, these retain the same direction throughout the matrix grain and also pass through the darker contrast regions. These

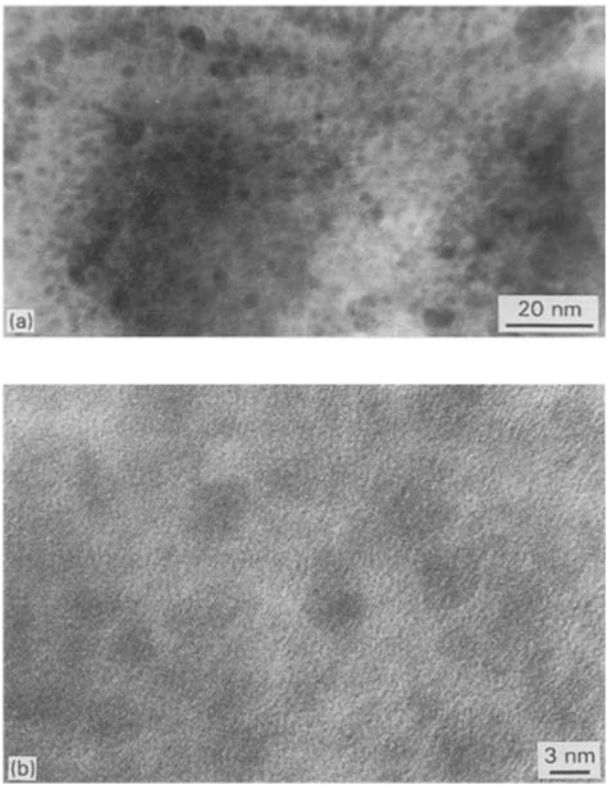

Figure 4 Bright-field micrographs of a sample of $Cu_{94}Co_6$ annealed at 600 °C, showing weak contrast features (a). In (b) the Cu lattice fringes traverse the weak contrast features.

regions may be a post-milling artefact but it is also possible that they are the products of a clustering process; they have the shape and size observed by Rabedeau *et al.* [24]. Moreover, they are coherent with the main lattice and so will not give rise to separate reflections, which is in agreement with experiment. However, a problem does arise with this interpretation in so far as Co has a smaller atomic scattering factor for electrons than Cu. Hence, a local excess of Co atoms should result in a diminution of electron scattering, whereas the opposite situation appears to prevail here. It is perhaps interesting to mention here that recent bright-field micrographs obtained from a sputtered 50% Ni–Fe–50% Ag multilayer, which had been thinned by ion-milling, also showed dark-contrast features similar to those observed in the present work [28].

It must be admitted that the inconclusive outcome of the electron microscope investigations with regard to the presence of clusters is disappointing, particularly so as the interpretation of the magnetic results (below) is predicated on their existence. This ambivalence of testimony does, however, accord with previous literature. As stated above, Rabedeau *et al.* [24] were unable to obtain direct, electron microscope confirmation of Co-rich clusters in as-prepared and annealed films of a $Co_{16}Cu_{84}$ alloy – although they yielded to an alternative technique. On the other hand, Berkowitz *et al.* [29] do claim to observe microscopically such clusters in annealed, sputtered $Co_{19}Cu_{81}$ films. In their report on sputtered $Co_{22}Cu_{78}$ granular films, Sand *et al.* [30] clearly show bright-field micrographs of Co granules about 10 nm in diameter embedded in an Ag matrix. In this case, the dissimilar scattering factors for Co and Ag lend themselves more easily to microscope observation than Co and Cu. It is of interest to note that in these CoAg films, the Co granules which have the lower scattering factors are in dark-contrast. On this basis, the small, dark features in Fig. 4(b) could be clusters of Co-rich material. The weak contrast may be due to low crystalline order as suggested by Wan *et al.* [22] in their study of FeAg alloys.

3.2. Magnetic measurements

Fig. 5(a) shows the variation of remanence as a function of temperature for a $Cu_{94}Co_6$ sample. These results were determined from the appropriate hysteresis loops, when a field of up to 5 T was applied at each temperature. We shall refer to these measurements of remanence as hysteresis loop remanences (HLRs). The maximum blocking temperature, T_B, of the sample is determined as being that temperature at which the extrapolated remanence intercepts the temperature axis; for the unannealed sample, this yields a value of T_B equal to 55 ± 5 K.

It is interesting to compare this temperature dependence of the remanence, and the associated maximum blocking temperature, with that determined from a different, but commonly employed, technique. Fig. 5(b) shows the temperature dependence of the

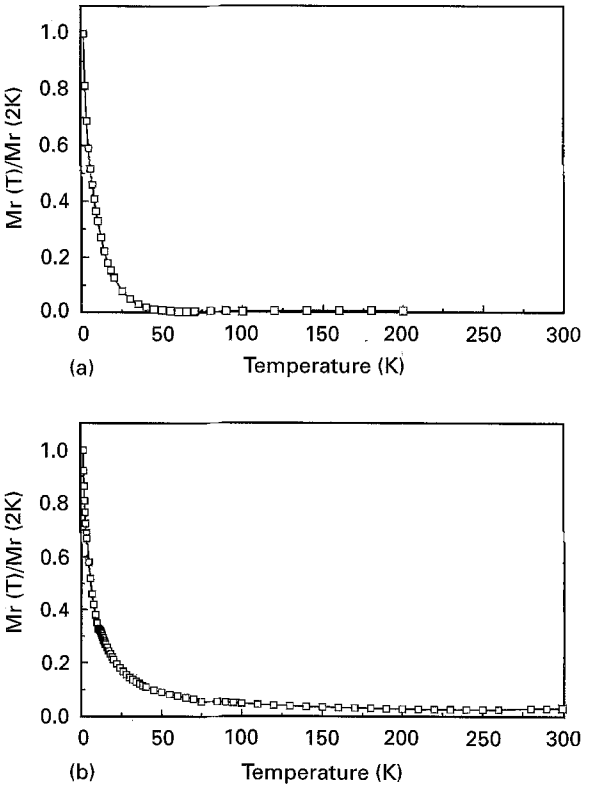

Figure 5 Temperature dependence of the remanence for an unannealed $Cu_{94}Co_6$ film. (a) The values of remanence are derived from the corresponding hysteresis loops (HLR) where a field of 5 T was applied at each temperature. (b) The values of remanence (TRM) are derived by applying a field of 5 T at 2 K, removing the field and then slowly warming up the sample. In both experiments, the remanence is normalized to its value at 2 K.

so-called thermoremanence (TRM) of the same sample. This data was obtained by cooling the sample from room-temperature to 2 K in zero-field, applying a field of 5 T at this temperature, removing the field and measuring the remanence. The sample was then slowly warmed-up to room temperature, measuring the residual magnetization (TRM) without any re-application of the field. In contrast to the previous determination of the temperature dependence of the remanence (HLR), it is not easy to draw conclusions about the maximum blocking temperature, since the sample shows a small, but finite value of remanence even at 300 K. Such different behaviour is also seen in more concentrated CuCo alloys [31]. However, it is not suggested that this behaviour is a characteristic of the CuCo alloy system, but rather that it is general feature of the two different types of measurement. However, to the best of the authors' knowledge, attention has not previously been drawn to this effect by making both types of measurement on the same sample. We attribute the difference in behaviour of the two types of measurement to the influence of interaction effects since, clearly, in the absence of interactions, we should expect a coincidence between them. It is possible that, in the TRM measurement, when the external field is initially removed at the lowest temperature, the small magnetic particles are able to orient their magnetizations in such a manner as to form flux-closure loops which, nevertheless, give rise to a finite remanence; the associated energy has both a local and a global minimum. If the temperature is now increased without the application, and subsequent removal, of a field, these energetically, initially favourable configurations are undisturbed and remain in a metastable or local, as opposed to a global, energy minimum, which is only attained after a field-cycle in a full hysteresis loop.

Fig. 6 shows the variation of HLR as a function of anneal. In this sequence of measurements, the remanence was measured from a starting temperature of 5 K. On anneal at 200 °C, there is an increase both in the HLR at any temperature, and also an increase in the corresponding maximum blocking temperature to 100 ± 10 K. i.e. above this temperature, the sample exhibits SPM. There is also a corresponding increase in the value of the TRM at any given temperature.

Further anneals at 400 and 600 °C result in strong increases in the remanence, with the HLR exhibiting a finite value at 300 K; the coercivity also exhibits a similar strong increase on anneal [31]. This behaviour is in general agreement with the work of Dieny *et al.* [6] who, in an investigation of melt-spun CuCo ribbons, found a particle size of 25 nm after a 10 min anneal at 950 K. They also observed a drastic increase in the magnetization on annealing between 650 and 750 K, which they were able to associate with structural changes in their ribbons due to the coalescing and formation of larger Co precipitates.

Fig. 7 shows the high- and low-field hysteresis loops, measured at 5 K, of a Cu_{94} Co_6 film both before any anneal and also after a final anneal at 600 °C. For the unannealed sample, a very narrow loop is observed, together with non-saturation of the magnetization, even in a field of 5 T. On anneal at intermediate temperatures, there is a gradual change in the shape of the loop. The hysteresis loop after anneal at 600 °C is much squarer, has a larger area and the magnetization saturates in a field of about 1 T. There is also a marked increase in the value of the magnetization at any given field.

Fig. 8 gives the variation of magnetization of a sample as a function of applied field, at a temperature of 5 K and its variation on anneal. The behaviour gradually changes from non-saturation, in the case of

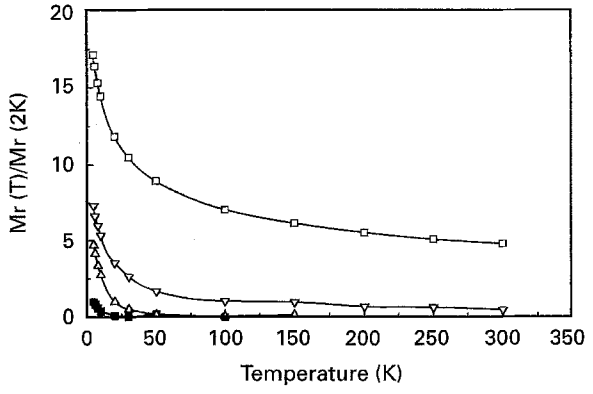

Figure 6 Temperature dependence of the remanence (HLR) for a $Cu_{94}Co_6$ sample as a function of anneal. Values are normalized to that of the unannealed sample at 5 K. ■ no anneal; Δ 200 °C; ∇ 400 °C; □ 600 °C.

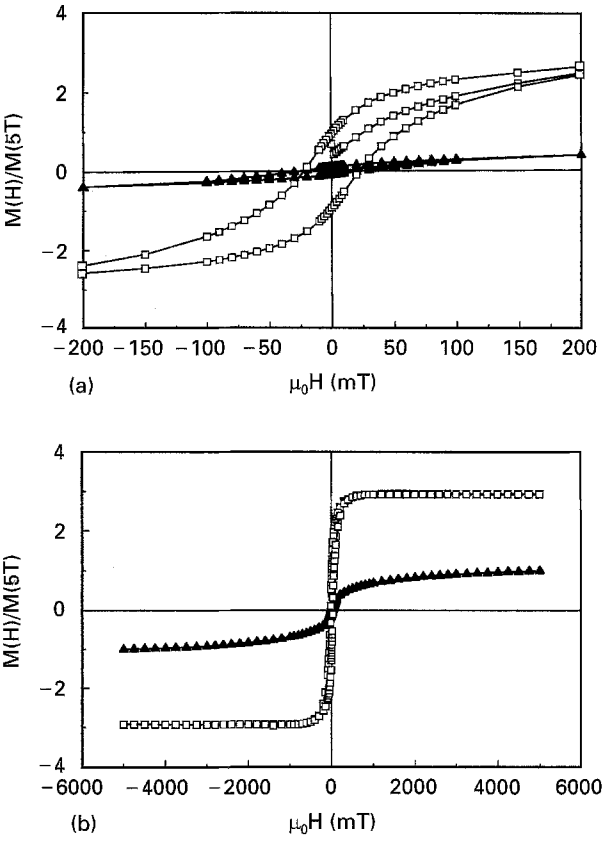

Figure 7 Hysteresis loop for an unannealed $Cu_{94}Co_6$ film measured at 5 K. (a) low-field, (b) high-field. The magnetization has been normalized to its value at 5 T for the unannealed sample. ▲ no anneal; □ 600 °C.

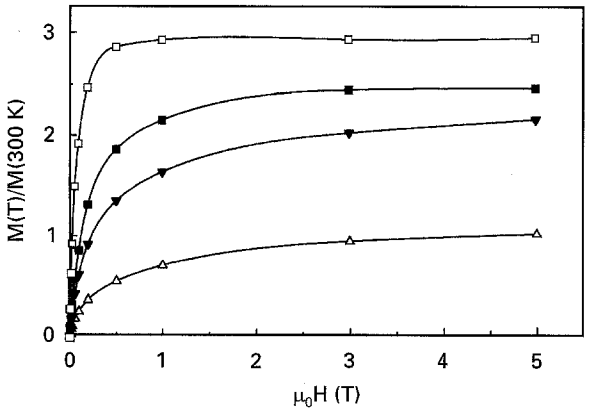

Figure 8 Magnetization of a $Cu_{94}Co_6$ film as a function of the magnetic field and measured at a temperature of 5 K. The results have been corrected for the contribution of the diamagnetic Cu substrate and are normalized to the value of the magnetization for the unannealed sample at a temperature of 300 K and a field of 5 T. △ no anneal; ▼ 200 °C; ■ 400 °C; □ 600 °C.

the unannealed sample, to a state where saturation is achieved in the 400 and 600 °C annealed samples in gradually lower values of applied field. Previous measurements on the unannealed sample [17] showed that even at temperatures in the range 150 to 300 K, temperatures well above T_B (55 ± 5 K), the films did not exhibit pure SPM, since plots of magnetization as a function of reduced field (H/T) did not superimpose; such scaling is a crucial test of SPM. This behaviour correlates well with the observation of a finite remanences (TRM) even at 300 K, in unannealed samples (Fig. 5b) and which we have earlier attributed to interaction effects.

Our interpretation of the results is based on the fact that in the unannealed sample, there must be a distribution of Co-rich particles in the Cu-rich matrix, not withstanding the lack of direct evidence from TEM or diffraction. These particles have blocking temperatures which range from well below the minimum temperature of 2 K attained in the present work, and corresponding to both isolated Co atoms and very small Co-rich particles, up to particles with blocking temperatures of 55 ± 5 K. If we assume a value of 5.55×10^{17} eV cm^{-3} for the value of K_A for f.c.c. Co [32] for these particles (the exact value for K_A is somewhat arbitrary, since presumably both shape and strain anisotropy play an important role) and use the Livingstone and Bean expression [33] $K_A v = 25 k_B T_B$, where v is the particle volume, we are able to estimate a maximum particle diameter of 7 nm. The presence of the very small Co particles in the Cu-rich matrix is the reason for the observation that, in the unannealed sample, saturation is not achieved (Fig. 7) even in a field of 5 T. On anneal, there is a diffusion of the isolated Co atoms to the Co-rich particles to produce a "ripening" effect, i.e. a growth of the Co-rich particles. Thus, this increase in the particle size results in a corresponding increase in blocking temperature and a larger value of remanence. The absence of the isolated Co atoms, and also the smaller, Co-rich particles in the annealed sample, is also an explanation for the change in shape of the hysteresis loop, since it is the smaller SPM particles which produce the non-saturation, whereas the larger particles give rise to the magnetic saturation.

After anneal at 400 °C the films become ferromagnetic, exhibiting a finite remanence as determined by HLR, even at room temperature (Fig. 6). More precisely, it seems that after anneal at 400 °C, part of the film becomes ferromagnetic, even at 300 K. This means that, after anneal, large Co-rich particles are formed in which a multi-domain state exists. Consequently, the size of the Co particles must be not less than 50–70 nm [34].

In order to investigate the influence of anneal on particle size, we have performed ZFC/FC measurements on the samples. Fig. 9(a) shows the results for

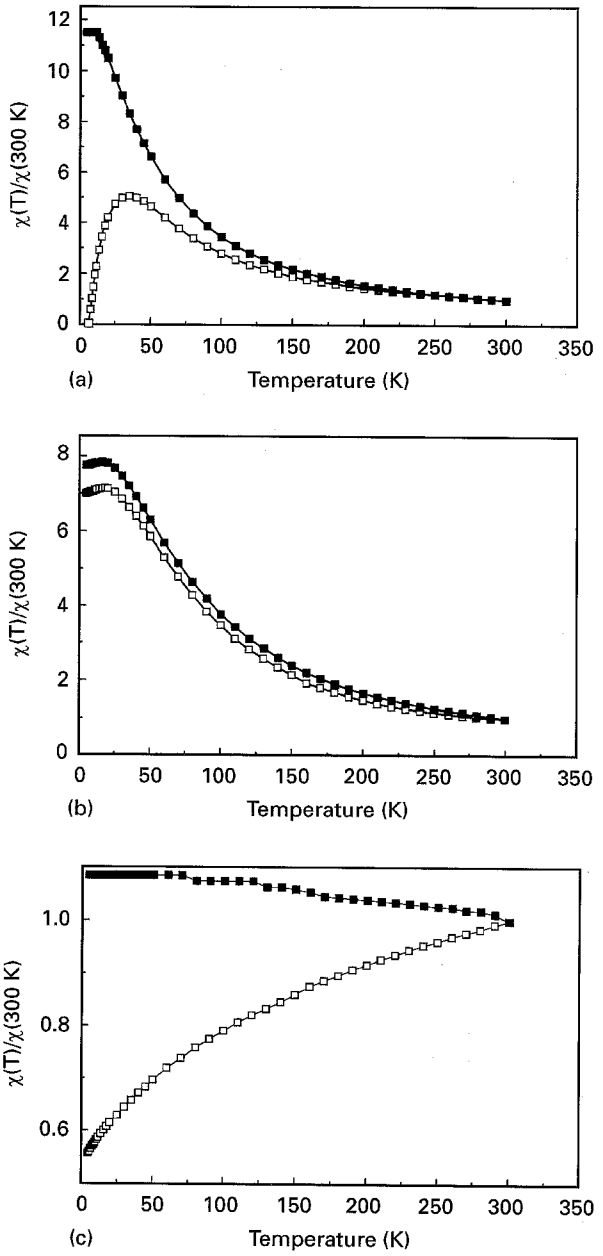

Figure 9 Magnetization of a $Cu_{94}Co_6$ film as measured in a field of 5 mT. The lower curve (□) is for the film initially cooled to 5 K in zero magnetic field (zero-field-cooled, ZFC), while the upper curve (■) is for the sample cooled in the measuring field 5 mT (field-cooled, FC). The results are normalized to the values of the magnetizations at 300 K. (a) unannealed sample; (b) annealed 30 min at 400 °C; (c) annealed 30 min at 600 °C.

the unannealed sample. Here, the maximum in the ZFC curve, which is related to the mean particle-size, occurs at 35 K and the bifurcation between the ZFC and FC curves at 250 K. The position of the bifurcation is generally taken to be an indication of the maximum blocking temperature of the sample [35]; this corresponds to particles of diameter 12 nm.

Although ZFC/FC measurements have been made on samples after anneal at each temperature, since the results for the 200 °C anneal are intermediate between the unannealed and the 400 °C sample, they will not be given here. The ZFC/FC curves for the 400 °C annealed sample (Fig. 9(b)) exhibit a strongly enhanced value of magnetization with the peak in the ZFC curve occurring at 20 K, whereas the bifurcation is at 300 K. This anomalous shift of the ZFC peak to lower temperatures on anneal is unexpected, since we would expect a growth in particle size, as is indicated by the increase of the remanence (Fig. 6) to shift the peak to higher temperatures. Such behaviour, however, has also been observed by Berkowitz *et al.* [36] and by Slade *et al.* [37] in CoAg granular alloys prepared by d.c. sputtering, when it was suggested that this effect could reflect a depletion of Co in the matrix, shifting the freezing temperature of the disordered matrix to lower values [36]. A similar effect has also been observed in a melt-spun $Cu_{85}Co_{15}$ alloy [25], although not in $Cu_{95}Co_5$ [26].

After a final anneal at 600 °C (Fig. 9(c)) no maximum is observed in the ZFC curve, which suggests that it lies outside the temperature range of the measurements and, on cooling from 300 K, there is an immediate divergence between the ZFC and FC curves. This indicates that both the peak in the ZFC curve and the bifurcation temperature are well above 300 K, corresponding to a particle size of greater than 15 nm. We subsequently extended the measurements on the 600 °C annealed sample up to 600 K, but were still unable to detect a peak in the ZFC curve.

In measurements made well above the blocking temperature of the samples, in the SPM region, we expect to see a Curie–Weiss-like behaviour of the susceptibility, χ, of the film. ie $\chi \propto (T - T_{int})^{-1}$, where T_{int} is an interaction temperature which may be positive or negative, depending upon the nature of the interparticle interaction [35, 38, 39]. In order to investigate this, in Fig. 10 we have plotted the reciprocals of the FC curves as a function of temperature for the unannealed and 400 °C annealed samples. Plotting the FC curve, rather than the ZFC curve, has the advantage that, since the FC curve is both reversible and reproducible, whereas the ZFC is reproducible but irreversible, we are able to eliminate blocking effects and therefore only have to consider interaction effects. By extrapolation of the high temperature, linear region of this curve to zero moment, we obtain an interaction temperature, T_{int}, of 20 ± 2 K for the unannealed sample, whereas for the 400 °C annealed sample, we obtain a value of 50 ± 5 K. If we define an interaction energy by the product $k_B T_{int}$ then there is an increase in this quantity from 1.7×10^{-3} eV in the unannealed sample to 9.0×10^{-3} eV after anneal at 400 °C.

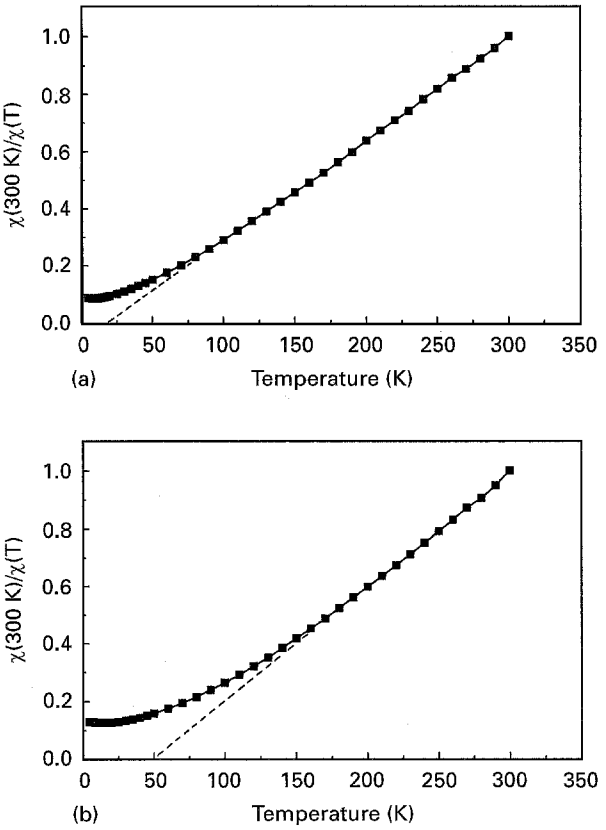

Figure 10 Temperature dependence of the reciprocal of the FC susceptibility of a $Cu_{94}Co_6$ sample normalized to its value at 300 K. (a) no anneal, the data is that of Fig. 9(a); (b) annealed to 400 °C, the data is that of Fig. 9(b).

4. Conclusions

In summary, measurements have been made of the influence of anneal on the magnetic properties of the heterogeneous alloy, $Cu_{94}Co_6$, which has been produced by electrode position. Despite the relatively low Co concentration, this film does not exhibit pure superparamagnetism and interaction effects have to be taken into account. For the unannealed samples, the remanence, as measured via conventional hysteresis loops, vanishes at 55 ± 5 K, which corresponds to the maximum blocking temperature of the superparamagnetic particles and suggests a maximum particle diameter of 7 nm; an interaction temperature of 20 ± 2 K is determined from low-field susceptibility measurements, which indicates the presence of positive, ferromagnetic-like interactions. This determination of the temperature dependence of the remanence is contrasted with that obtained from measurement of the thermoremanence. On anneal, there is a strong increase in both the remanence and maximum blocking temperature of the sample, with an interaction temperature of 50 ± 5 K after anneal at 400 °C. On anneal at 600 °C, the size of the particles is such that they are still blocked at 300 K and the sample shows a ferromagnetic behaviour.

Transmission electron microscopy studies of the films proved to be problematic. This was due, to some extent, to the difficulty encountered in thinning the samples for microscopy using the technique of ion-milling, which may have introduced post-deposition artefacts. The samples indicated a complex structure

with no unambiguous evidence for isolated pure Co particles in a Cu-rich matrix, the structure of the films being influenced, to a large degree, by the crystal structure of the substrate.

It is concluded, from a comparison with the numerous recent publications on the CuCo alloy system, on samples which have been prepared by several different routes that, whereas the general behaviour of the system is common to all preparation routes, the detailed magnetic behaviour of the material depends strongly upon the sample microstructure.

Acknowledgements

Thanks are due to Mr Brian Ashworth and Dr G. J. Sinclair for sample thinning and help with the electron microscopy. We are grateful to Professor G. A. Gehring for a critical reading of the manuscript and to Professor R. W. Chantrell for helpful discussions. One of us (V.M.F.) wishes to express his gratitude to the Royal Society for the award of a European Research Fellowship, during the tenure of which this work was partly carried out. Acknowledgement is also made of EPSRC support under grant numbers GR/H63395 and GR/J25338.

References

1. S. M. THOMPSON, J. F. GREGG, C. R. STADDON, D. DANIEL, S. J. DAWSON, K. OUNADJELA, J. HAMMANN, C. FERMON, G. SAUX, K. O'GRADY, S. J. GRIEVES, J. M. D. COEY and A. FAGAN, *Phil. Mag.* **B68** (1993) 923.
2. F. CONDE, C. GÓMEZ-POLO and A. HERNANDO, *J. Magn. Magn. Mater.* **138** (1994) 123.
3. J. WECKER, R. VON HELMHOLT and L. SCHULTZ, *Appl. Phys. Lett.* **62** (1993) 1985.
4. Y. HUAI, M. CHAKER, H. PÉPIN, S. BOILY, X. BIAN, R. W. COCHRANE, *J. Magn. Magn. Mater.* **136** (1994) 204.
5. R. J. GAMBINO, T. R. MCGUIRE, J. M. E. HARPER and C. CABRAL Jr., *J. Appl. Phys.* **75** (1994) 6909.
6. B. DIENY, A. CHAMBEROD, C. COWACHE, J. B. GENIN, S. R. TEIXEIRA, R. FERRE and B. BARBARA, *J. Magn.* and *Magn. Mater.* **135** (1994) 191.
7. G. XIAO and J.-Q. WANG, *J. Appl. Phys.* **75** (1994) 6604.
8. S. ZHANG, *Appl. Phys. Lett.* **61** (1992) 1855.
9. S. ZHANG and P. M. LEVY, *J. Appl. Phys.* **73** (1993) 5315.
10. R. E. CAMLEY and J. BARNAS, *Phys. Rev. Lett.* **63** (1989) 664.
11. B. L. JOHNSON and R. E. CAMLEY, *Phys. Rev.* **B 44** (1991) 9997.
12. J. SHI, R. C. YU, S. S. P. PARKIN and M. B. SALAMON, *J. Appl. Phys.* **73** (1993) 5524.
13. J. SHI, E. KITA, I. XING and M. B. SALAMON, *Ibid.* **73** (1993) 5524.
14. K. OUNADJELA, A. HERR, R. POINSOT, J. M. D. COEY, A. FAGAN, C. R. STADDON, D. DANIEL, J. F. GREGG, S. M. THOMPSON, K. O'GRADY and S. GRIEVES, *Ibid.* **75** (1994) 6920.
15. Y. UEDA and M. ITO, *Japan. J. Appl. Phys.* **33** (1994) L1403.
16. H. J. BLYTHE and V. M. FEDOSYUK, *Phys. Status. Solidi (a)* **146** (1994) K13.
17. H. J. BLYTHE and V. M. FEDOSYUK, *J. Phys.: Cond. Mat.* **7** (1995) 3461.
18. M. ALPER, K. ATTENBOROUGH, R. HART, S. J. LANE, D. S. LASHMORE, C. YOUNES and W. SCHWARZACHER, *Appl. Phys. Lett.* **63** (1993) 2144.
19. S. K. J. LENCZOWSKI, C. SCHÖNENBERGER, M. A. M. GIJS and W. J. M. DE JONGE, *J. Magn. Magn. Mater.* **148** (1995) 455.
20. H. J. BLYTHE and V. M. FEDOSYUK, *Ibid.* **155** (1996) 352.
21. R. W. CHANTRELL, G. N. COVERDALE, M. EL-HILO and K. O'GRADY, EMMA, Vienna, 1995, *Ibid.* In press.
22. H. WAN, A. TSOUKATOS, G. C. HADJIPANAYIS, Z. G. LI and J. LIU, *Phys. Rev.* **B49** (1994) 1524.
23. E. KNELLER, *J. Appl. Phys.* **33S** (1962) 1355.
24. T. A. RABEDAU, M. F. TONEY, R. F. MARKS, S. S. P. PARKIN, R. F. C. FARROW and G. R. HARP, *Phys. Rev.* **B48** (1993) 16810.
25. R. H. YU, X. X. ZHANG, J. TEJADA, M. KNOBEL, P. TIBERTO and P. ALLIA, *J. Phys.: Cond. Mat.* **7** (1995) 4081
26. *Idem., Zeit. für Physik* **98** (1995) 447.
27. M. P. DANIEL, D. S. LASHMORE and L. H. BENNETT, in "Magnetic multilayers", edited by L. H. Bennett and R. E. Watson (World Scientific Press, London, 1994) p. 373.
28. S. J. GUILFOYLE, private communication.
29. A. E. BERKOWITZ, J. R. MITCHELL, M. J. CAREY, A. P. YOUNG, S. ZHANG, F. E. SPADA, F. T. PARKER, A. HUTTEN and G. THOMAS, *Phys. Rev. Lett.* **68** (1992) 3745.
30. H. SANG, S. Y. ZHANG, H. CHEN, G. NI, J. M. HONG, X. N. XHAO, Z. S. JIANG and Y. W. DU, *Appl. Phys. Lett.* **67** (1995) 2017.
31. H. J. BLYTHE and V. M. FEDOSYUK, to be published.
32. R. S. TEBBLE and D. J. CRAIG, "Magnetic materials" (J. Wiley, Interscience, London, 1969).
33. C. P. BEAN and J. D. LIVINGSTONE, *J. Appl. Phys.* **30** (1959) 120S.
34. E. KNELLER, "Ferromagnetismus" (Springer Verlag, Berlin, 1962).
35. M. EL-HILO, K. O'GRADY and R. W. CHANTRELL, *J. Magn. Magn. Mater.* **114** (1992) 295.
36. A. E. BERKOWITZ, J. R. MITCHELL, M. J. CAREY, A. P. YOUNG, D. RAO, A. STARR, S. ZHANG, F. E. SPADA, F. T. PARKER, A. HUTTEN and G. THOMAS, *J. Appl. Phys.* **73** (1993) 5320.
37. S. B. SLADE, F. T. PARKER and A. E. BERKOWITZ, *Ibid.* **75** (1994) 6613.
38. M. EL-HILO, K. O'GRADY and R. W. CHANTRELL, *J. Magn. Magn. Mater.* **114** (1992) 307.
39. *Idem., Ibid.* **117** (1992) 21.

Received 8 December 1995
and accepted 15 January 1996